RBRH

Revista Brasileira de Recursos Hídricos
Brazilian Journal of Water Resources
Versão On-line ISSN 2318-0331
RBRH, Porto Alegre, v. 25, e9, 2020
Scientific/Technical Article

https://doi.org/10.1590/2318-0331.252020190061

Scenarios of climate change effects in water availability within the patos Lagoon's Basin

Cenários de mudanças climáticas na disponibilidade hídrica na bacia hidrográfica transfronteiriça da Laguna dos Patos

Raíza Cristóvão Schuster[1], Fernando Mainardi Fan[1] & Walter Collischonn[1]

[1]Universidade Federal do Rio Grande do Sul, Porto Alegre, RS, Brasil
E-mails: schuster.raiza@gmail.com (RCS), fernando.fan@iph.ufrgs.br (FMF), collischonn@iph.ufrgs.br (WC)

Received: May 13, 2019 - Revised: August 18, 2019 - Accepted: November 12, 2019

ABSTRACT

The decision-making processes involving water resources in Brazil and in neighboring countries have been based solely on analyses of the historical behavior of hydroclimatological variables. However, this may lead to inappropriate strategies in regards to the use of natural resources, since the impact of future climate change may significantly affect the availability of water resources. This study proposes an analysis of the variation in water availability of basins within the Patos Lagoon contribution area, which may be a consequence of climatic changes predicted by CMIP5 (Coupled Model Intercomparison Project Phase 5) models, published in the most recent International Panel on Climate Change (IPCC) report. Two 30-year periods were simulated, from 2006 to 2035 and from 2051 to 2080, through the MGB-IPH hydrological model, considering two extreme greenhouse gas scenarios and twenty climate change models. A tendency of increase of the flows was verified in the simulated basin, since over 60% of the simulations indicated some percentage of average flow increase across all discretized modeling units. The analysis of the simulation results indicated that the data from climatic models HadGEM2-ES and GFDL-CM3 used as input in the hydrological model are the ones that respectively provide upper and lower flow thresholds for the ensembled simulations. A joint evaluation of the results generated by these two models, associated with the scenario of high greenhouse gas emissions, is capable of covering extreme flow scenarios making predictions considering climate change in the Patos Lagoon's basin. Whereas the results provided by bcc-csm1, BNU-ESM and CNRM-CM5 are similar to the median of the ensemble of simulations generated by all models evaluated in this research. In addition, the northernmost region of the study area was identified as having the highest sensitivity to climate change, as projected by global models of CMIP5 published in AR5.

Keywords: Climate change; Patos Lagoon's basin; Water availability.

RESUMO

Os processos de tomada de decisão que envolvem recursos hídricos no Brasil e países vizinhos vêm se baseando unicamente em análises do comportamento histórico de variáveis hidrológicas e climatológicas. Entretanto, isto pode levar a estratégias equivocadas relacionadas ao uso dos recursos naturais, pois o impacto das mudanças climáticas no comportamento das vazões futuras pode alterar consideravelmente a disponibilidade de recursos hídricos. Na presente pesquisa foi realizada uma análise da variação das disponibilidades hídricas de bacias hidrográficas contidas na área de contribuição à Laguna dos Patos, Rio Grande do Sul - Brasil, e Uruguai, que pode ser consequência das mudanças climáticas previstas por modelos globais do CMIP5 (Coupled Model Intercomparison Project Phase 5), publicados no mais recente relatório do IPCC (International Panel on Climate Change). Dois períodos futuros de 30 anos foram simulados, de 2006 a 2035 e de 2051 a 2080, utilizando o modelo hidrológico MGB-IPH, considerando dois cenários extremos de emissões de gases de efeito estufa e vinte modelos climáticos. Foi possível verificar uma tendência de aumento das vazões na bacia hidrográfica simulada, pois mais de 60% das simulações realizadas indicou algum percentual de aumento de vazões médias em todas as unidades de discretização modeladas. A análise dos resultados das simulações indicou que os dados dos modelos climáticos HadGEM2-ES e GFDL-CM3 utilizados como dados de entrada no modelo hidrológico são os que fornecem, respectivamente, limiares superiores e inferiores de vazão do conjunto de resultado simulados. A avaliação conjunta dos resultados gerados por estes dois modelos, associados ao cenário de altas emissões de gases de efeito estufa, é capaz de gerar cenários extremos de vazões que são projetados para o futuro considerando as mudanças climáticas na bacia hidrográfica da Laguna dos Patos. Já os resultados fornecidos

pelos modelos bcc-csm1-1, BNU-ESM e CNRM-CM5 são similares à mediana do conjunto das simulações geradas por todos os modelos avaliados nesta pesquisa. Além disso, a região mais ao norte da área de estudo foi identificada como as que apresenta maior sensibilidade às mudanças climáticas projetadas pelos modelos globais do CMIP5.

Palavras-chave: Mudanças climáticas; Bacia hidrográfica da Laguna dos Patos; Disponibilidade hídrica.

INTRODUCTION

Decision-making processes involving water resources in Brazil have been based on analyses of the historical behavior of variables such as rain, discharge, temperature, etc. This occurs both in the management of basins as in the building of hydraulic constructions, dams for the public supply of water and generation of power, for example. However, the use of time series based on observations of the past may lead to mistaken strategies in regards to the use of natural resources, since the impact of climate change in the behavior of future rainfall may considerably alter the availability of water resources (Lima et al., 2014).

Considering that over the last two decades panels of scientists have been alerting about the process of climate change, which are brought about by atmosphere concentration of greenhouse gases, it is necessary that water resource management instruments be ready for the impact that these changes might engender.

The International Panel on Climate Change (IPCC) evaluates, interprets and gathers relevant information concerning climatic changes and provides periodic reports intended to support political decisions. These reports highlight the importance of taking climate change into account in the global management sphere (Pachauri & Meyer, 2014).

In Brazil, water resource management instruments have been instituted by the Federal Law nº 9.433 (Brasil, 1997), January 8th, 1997, known as "Water Resources National Policy". These instruments are the Water Resources Plans; the framework of water bodies in classes, according to their compelling uses; the granting of rights to the use of water resources; the charging for the use of water; the compensation of municipalities; and the Information System on Water Resources.

Even before the passing of Federal Law nº 9.433, three of the countries' states already had water resource legislations in place. The pioneering state was São Paulo, which established guidelines for the State Policy for Water Resources and the Integrated Water Management System on December 30th, 1991, through the State Law nº 7.663 (São Paulo, 1991). The second was the Water resources law of the state of Ceará, established by State Law nº 11.996 on July 24th(Ceará, 1992).

Rio Grande do Sul (RS) was the third state to adopt its own water resource legislation, the State Law nº 10.350, on December 30th, 1994 (Rio Grande do Sul, 1995). This legislation envisions the proposition, execution and updating of the River Basin Plans (PBH - Planos de Bacia Hidrográfica) as objectives of the State System of Water Resources. The River Basin Plans aim to operationalize, in the context of each river basin, the provisions in the State Plan for Water Resources over a four-year period. Reconciling the qualitative and the quantitative aspects, thus ensuring that the goals and uses envisioned by the State Plan for Water Resources are simultaneously achieved, with tangible and continued improvements of the qualitative aspects in bodies of water (Rio Grande do Sul, 1995).

The PBH that have already been drafted in the RS state feature qualitative and quantitative water balances over different scenarios, comparing current and future water uses with water availability, without considering that availability may vary in the future, unless due to increased discharge by reservoirs.

Nonetheless, many recent studies have shown that the impact of climatic changes could prove to be substantially relevant regarding water availability. In the Brazilian context we can name works such as shown in Table 1.

Regarding these studies, we highlight that in the majority of them limited amounts of climate models were used for the analyses, under the pretext that these models would be representative of the whole. Yet, there are few scientific hydrology papers highlighting information such as: what would be the most representative models in regards to the distribution of forecasts within a region? Within the universe of possible climate models that can be used in hydrological projections, how are they distributed? Those are the very answers that are interesting in the context of water resource planning, seeing as models fairly identified as representative could be the ones to demanded by environmental institutions for technical local studies. Thus, decreasing the effort (as well as the costs) in obtaining relevant information with respect to possible impacts of climate change.

Amorim & Chaffe (2019) propose a ranking procedure to evaluate 42 studies that integrate climate models into hydrological modeling in the Brazilian territory. The authors realized that multi-model ensemble approach and evaluation of models are under limited application in Brazil, and that high flows are more likely to increase in Southern Brazil.

Continuing the overview of the Brazilian background, Borges & Chaffe (2019) have recently evaluated 32 scientific documents that compose the climate model outputs with hydrological modeling in case studies within the Brazilian territory. Highlighting the fact that several drainage basins do not possess climate change projection analysis. Among the basins listed by Borges & Chaffe (2019), the Patos Lagoon's (Laguna dos Patos) basin stands out. Located in Brazil (state of Rio Grande do Sul) and Uruguay, it is the most economically relevant hydrographic basin in the Rio Grande do Sul state (Lopes, 2017).

Within this framework, an analysis of the variance of water availability was undertaken in the current research. The study accounted through reference discharges in basins contained in the Patos Lagoon's contribution area, which are the consequence of climate changes forecast by CMIP5 (Coupled Model Intercomparison Project Phase 5) global models, published in the most recent IPCC report. The objective of the research was to assess future climate change scenarios predicted by global models of the fifth IPCC report in water availability indexes within the hydrographic basins that drain into the Patos Lagoon; and identifying what climate models would be the most representative of result distribution in the region.

STUDY AREA

The Patos Lagoon's watershed has around 182 thousand km^2 (Figure 1), 82% in Brazilian territory and the remaining area in Uruguay. It covers an immense diversity of types of ground coverage, such as agriculture, urban occupancy, industrial and natural vegetation. According to Koppen climate classification, this basin has warm oceanic / humid subtropical climate.

Patos Lagoon watershed contains the Jacuí River basin, which, together with the Gravataí, Sinos and Caí rivers, form the Jacuí Delta, which flows into Guaíba Lake, which flows into Patos Lagoon. Camaquã river and São Gonçalo Canal sub-basins flow

Table 1. Studies using climatic models to evaluate water availability change in the future.

Studie	Study area	Hydrological Model	Climate data
Nóbrega et al. (2011)	*Grande River basin*	*MGB-IPH*	*6 AR4 models under A1b, A2, B1, B2 emissions scenarios*
Adam And Collischonn (2013)	*Ibicuí River Basin, in Southern Brazil*	*MGB-IPH*	*20 AR4 models under A1B, A2 and B2 emissions scenarios*
Adam et al. (2014)	*Paraná River Basin*	*MGB-IPH*	*4 members of the original ETA-CPTEC model under A1B emissions scenario*
Lima et al. (2014)	*Amazon, Tocantins, Paraíba do Sul, Parnaíba, Paraná, Iguaçu, Taquari-Antas, Jacuí, Uruguay, Paraguay, Capivari and Itajaí*	*MGB-IPH and MGB-INPE*	*GFCM, MPEH, MRCG, HADCM, NCCC and ETA*
Tejadas et al. (2016)	*Magueira Lagoon in, Southern Brazil*	*IPH II*	*20 AR4 models under A2 and B2 emissions scenarios*
Sorribas et al. (2016)	*Amazon basin*	*MGB-IPH*	*5 AR5 models under RCP8.5 emissions scenario*
Alvarenga et al. (2016)	*Lavrinha spring basin, in southwestern Brazil*	*DHSVM*	*ETA coupled with the HadGEM2-ES model under AR5 RCP 8.5 emissions scenario*
Oliveira et al. (2017)	*Grande River basin*	*SWAT*	*2 AR5 models under RCP 4.5 and 8.5 emissions scenario*
Fernandes et al. (2017)	*Two reservoirs in the state of Ceará*	*SMAP*	*20 AR5 models under RCP 4.5 and RCP 8.5 emissions scenario*

Figure 1. Study area location.

directly into Patos Lagoon. Table 2 presents the study catchments general characteristics.

The basin possesses a large population and industrial concentration in some areas, causing great pressure on natural resources. Furthermore, the use of water for irrigation is very important, affecting the amount of water available for other uses within the basin (Pereira et al., 2012). Therefore, water resource planning studies are of great importance for this region.

The results of this research are evaluated at the outflow points of the Lagoon's main contributors: rivers Gravataí, Sinos, Caí and Baixo Jacuí, which drain to Lago Guaíba (Guaíba Lake), which drains to the northern portion of Patos Lagoon; Camaquã River, which drains west of the Lagoon's middle portion; and the São Gonçalo canal, which drains exactly south of Patos Lagoon. The results were also assessed at Patos Lagoon's watershed outflow into the Atlantic Ocean.

MATERIAL AND METHODS

Future climate data

Data from 20 climate models were used (Table 3), selected by development Group I from IPCC's AR5, made available through the German Climate Centre (DKRZ, Deutsches Klimarechenzentrum). Every usable model that possessed data for all necessary climate variables to implement the hydrological model in the CMIP database (precipitation, wind speed, relative air humidity, atmospheric pressure, solar radiation and temperature) was employed. Table 2 presents the models list.

The future climate variable data for South America are provided in regular point grids, that vary from model to model. We adopted the approach of considering the climate conditions prescribed by climate models in terms of anomalies of the variables of interest relative to current climate rather than taking its absolute values.

Both of the most extreme greenhouse gas emissions scenarios of the fifth IPCC report were considered: RCP 2.6, as a rigorous mitigation scenario, and RCP 8.5, with exceptionally high GEE emissions. These were the utilized scenarios since they indicate the variability to which the hydrographic basin will be subjected.

Two future 30-year periods were simulated to which AR5 climate models have been published: from 2006 to 2035, which in this paper is called "near future"; and from 2051 to 2080, which is named "distant future."

Hydrological model

This research used the hydrological model MGB-IPH prepared by Lopes et al. (2018), which simulates, in the same computational model, all basins that contribute to coastal lagoon complexes in Rio Grande do Sul.

Table 2. General characteristics of the study catchments.

Catchment	Area (10^3 km^2)	Average discharge (m^3/s)	Average precipitation (mm/year)
Gravataí	*2*	*66*	*1.414*
Sinos	*3,7*	*132*	*1.572*
Caí	*5*	*179*	*1.625*
Jacuí	*71*	*2.790*	*1.583*
Camaquã	*17*	*533*	*1.434*
São Gonçalo Canal	*57*	*1.670*	*1.285*

Table 3. CMIP climatic models employed.

Model	Institution
bcc-csm1.1	*Beijing Climate Center, China*
bcc-csm1.1m	
BNU-ESM	*Beijing Normal University, China*
CanESM2	*Canadian Centre for Climate Modeling and Analysis, Canada*
CNRM-CM5	*Centre National de Recherches Météorologiques, France*
IPSL-CMA5-LR	*Institut Pierre Simon Laplace, France*
IPSL-CMA5-MR	
CSIRO-Mk3.6.0	*Commonwealth Scientific and Industrial Research Organisation, Australia*
GFDL-CM3	*Geophysical Fluid Dynamic Laboratory, USA*
GFDL-ESM2G	
GFDL-ESM2M	
GISS-E2-H	*Goddard Institute for Space Studies, USA*
GISS-E2-R	
HadGEM2-AO	*Met Office Hadley Centre, United Kingdom*
HadGEM2-ES	
MIROC5	*Atmosphere and Ocean Research Institute, University of Tokyo, National Institute for Environmental Studies, & Japan Agency for*
MIROC-ESM	*Marine-Earth Science and Technology, Japan*
MIROC-ESM-CHEM	
MRI-CGM3	*Meteorological Research Institute, Norway*
NorESM1-M	*Norwegian Meteorological Institute, Norway*

Lopes et al. (2018) modeled Patos Lagoon through use of MGB-IPH, with terrain data acquired through a Digital Elevation Model (MDE) from the Shuttle Radar Topography Mission (SRTM) for the discretization of the simulated region into 2,627 unit-catchments, each representing an incremental drainage area from simulated reaches of water courses. Daily rainfall data series from 663 rain-stations, including seven Uruguayan stations, and daily air temperature data, relative air humidity, wind speed, atmospheric pressure and solar insolation from monitoring stations of the National Institute of Meteorology (INMET) were used as input for the model. The model performance for river discharge was considered coherent, especially in the north region of the basin (Lopes et al., 2018), with daily Nash-Sutcliffe efficiency coefficient values mostly over 0.6 and absolute BIAS lower than 10%. More details about the hydrological model can be found within Lopes et al. (2018) and Lopes (2017).

Discharge series resulting from the implementation of Lopes et al. (2018)'s model for the period of 1961 to 1990 were considered as a control scenario. The hydrological model was implemented for the simulation of each climate change scenario, taking climate variables into account for each model's future climate.

Methodological steps

Climate models used in this paper were not designed to provide the actual daily representation of future climate condition. Therefore, climate data is considered in terms of anomalies of the variables of interest relative to current climate rather than taking its absolute values, adopting the same methodology as in Bravo et al. (2014) and Adam & Collischonn (2013). The value of the anomaly between the data series estimated by the climate model over the control periods (1961-1990) and the simulation periods (2006-2035 and 2051-2080) were used to disturb the climate data series over the period of 1961 to 1990 of the INMET monitoring stations and the interpolated rainfall series for each unit-catchments based on data acquired from rain checkpoints.

A spatial downscaling was performed so as to meet the climate model's closest coordinates at each climate data station, and each hydrological modeling discretization unit. For each INMET station, the point closest to the climate model grid was selected, and the anomaly value was used to disturb the data series of temperature, humidity, wind speed, radiation, insolation and atmospheric pressure, thus generating future data for these variables. For each of the hydrological model's unit-catchments, the point closest to the climate model grid was selected, and the anomaly value was used to disturb the rainfall data series interpolated in modeling, generating future precipitation data series.

Therefore, through the use of the variables' historical data (from 1961 to 1990) as input for the hydrological model, a series of discharge data was created for the control period; and using the future data series as input, discharge data series were generated for future periods. Figure 2 presents an example of the methodological steps performed to generate discharge data to the control period (in blue) and to a near future period with RCP 2.6 using bcc-csm1.1 model (in red). Red steps from Figure 2 were performed for each one of the 20 climate models, with 2 RCP and for 2 future periods (2006-2035 and 2051-2080).

That is, 80 discharge series were generated for each of the 2,627 unit-catchments or drainage reaches. To smooth the analysis, considering the great quantity of generated data, the average discharge was calculated for the generated series over each period, scenario and climate model. They were subsequently compared to the control period's discharge averages.

The analyses of results were performed specifically at the outflow points of the rivers Gravataí, Sinos, Caí, Jacuí, Camaquã, São Gonçalo Canal and the Barra de Rio Grande, at the Patos Lagoon's outflow, and, spatially, through the origination of charts. Finally, an analysis of which models best represent the set distributions was carried out, providing the most extreme results and the medians within the analyzed set.

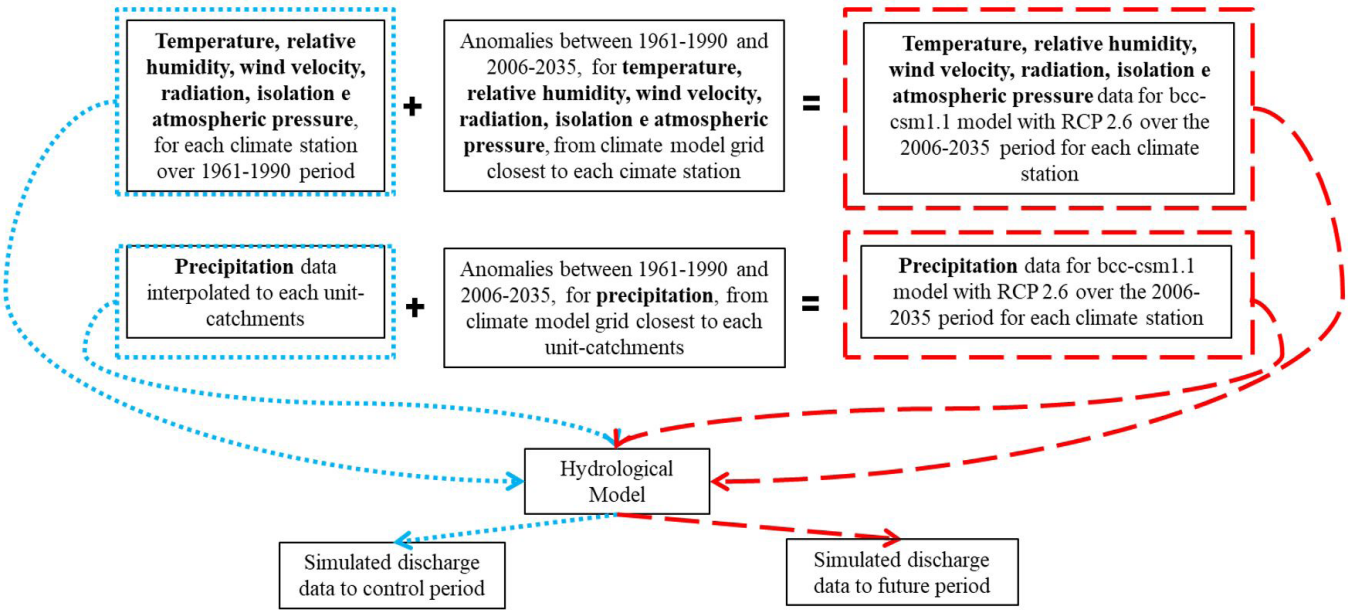

Figure 2. Methodological steps performed to generate discharge data to the control period (in blue) and to a near future period with RCP 2.6 using bcc-csm1.1 model (in red).

RESULTS AND DISCUSSION

Analysis in checkpoints

From Figures 3-6 are illustrated variations in average simulated discharge across the twenty climate models at their checkpoints for each considered scenario and period.

The chart at Figure 3 features average discharge variations for RCP 2.6, over the period of 2006 to 2035, and illustrates that the largest part of the models presents a tendency to increase discharge. The percentile of discharge variation values range between +23%, as verified at the outflow point of Caí and Camaquã watersheds, and -12%, verified at the outflow of the Jacuí river basin.

Still in regards to Figure 3, it is noted that models HadGEM-AO, HadGEM-ES and MRI-CGCM3 provide the highest increase in average discharge, being the only ones to surpass the 20% increase for some basins. On the other hand, the GFDL-CM3 model is the only one to be prone to decreased discharge across all checkpoints. Moreover, it is verified that a same model usually presents a tendency of discharges increasing across all basins, or a tendency of discharges decreasing across all basins. Only the CanESM2, CSIRO-Mk3-6-0, GFDL-ESM2G and MIROC-ESM display a tendency to increase in some checkpoints, and decrease in others.

Figure 4 exhibits average discharge variations for RCP 2.6 over the period of 2051 to 2080. Under this condition, where the emissions scenario is the same as in the previous figure, but the period is a more distant future, the tendency towards increased discharge is visually a bit stronger. The increased percentile variation range is shifted upwards, varying between +26% and

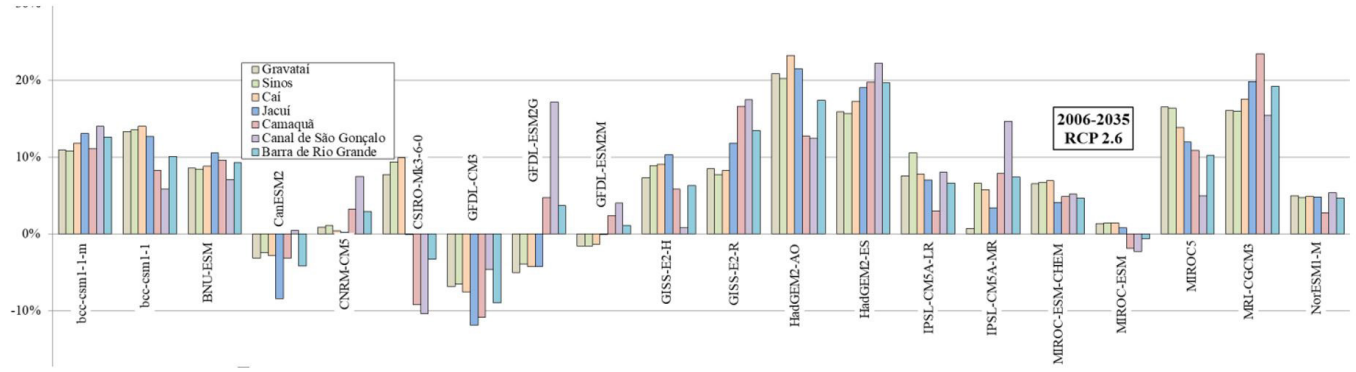

Figure 3. Average discharge variation at points of interest with RCP 2.6 over the 2006-2035 period.

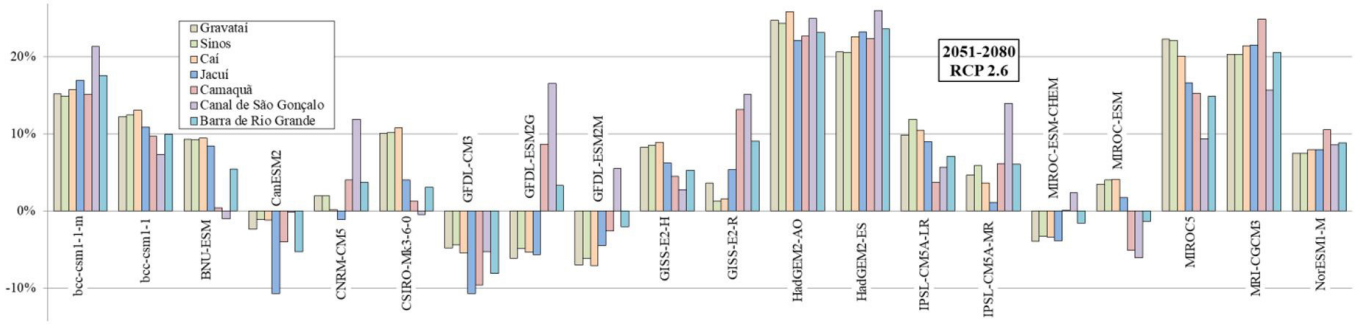

Figure 4. Average discharge variation at points of interest with RCP 2.6 over the 2051-2080 period.

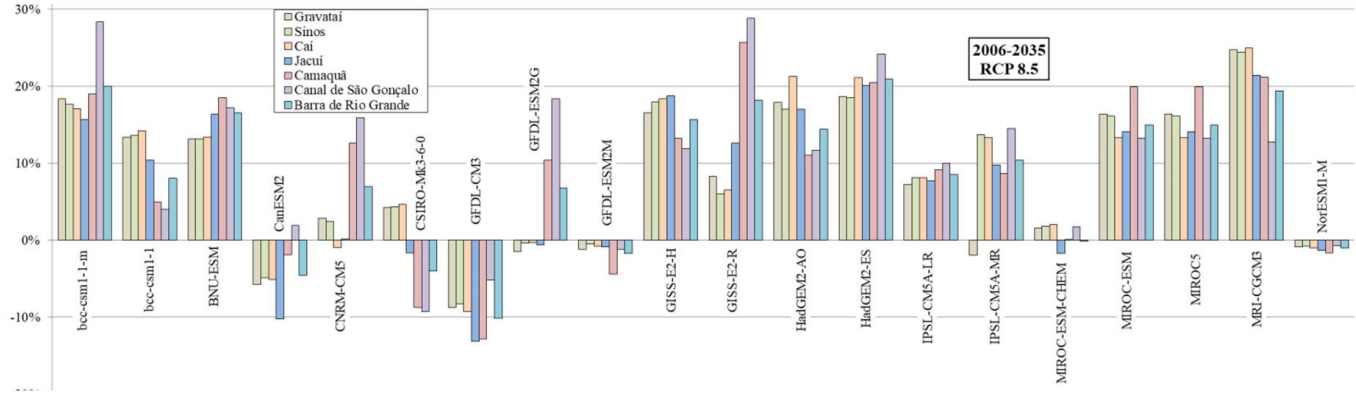

Figure 5. Average discharge variation at points of interest with RCP 8.5 over the 2006-2035 period.

-11%, and two other models reach deviations higher than 20% (bcc-csm-1-1m and MIROC5), apart from the three aforementioned. However, in this more distant future, a higher uncertainty is noticed in regards to the tendency of some models, once there is a higher quantity of models that exhibit a tendency to increase in some checkpoints, and a tendency to decrease in others.

Figure 5 features results for the scenario with the highest emissions (RCP 8.5) in a near future, from 2006 to 2035. In this situation, the range of variations is expanded, varying between +29% and -13%. In this graph, it is noticeable that at the outflow of coastal region watersheds (Camaquã river and São Gonçalo Canal), the largest tendencies towards average increased discharge are verified overall.

Figure 6 displays the most extreme emissions scenario (RCP 8.5) in a more distant future (from 2051 to 2080). In this situation are found the largest discharge variation extremes, which deviate at checkpoints between +57% and -22%. The largest increase variations were verified at the watershed outflow of the Caí River, and the most extreme decrease variations were verified at the outflow of the Jacuí river basin. The overall tendency towards increased average discharge is boosted under these conditions, where 12 of the 20 models display positive deviations over 20%. Still, out of the 140 pieces of data featured in this graph, only 20, representing around 14,3%, indicate negative discharge deviations.

To complement the analysis of data, some box plot diagrams were elaborated, presented from Figures 7-10. Through the analysis of the box plot diagrams, a tendency towards increased discharge is noticeable as dominating in the checkpoints of the posed scenarios and periods, since the rectangles in the diagrams are practically entirely found above the zero axis. On Figure 7, showing the results for checkpoints with RCP 2.6 over the period of 2006 to 2035, the interquartile range and the distance between the extremities of the whiskers indicate a small variation in values when compared to the Figure 8 and Figure 10 graphs, which feature results for the period between 2051 and 2080 with RCP 2.6 and 8.5, respectively, where the whisker length is considerably higher.

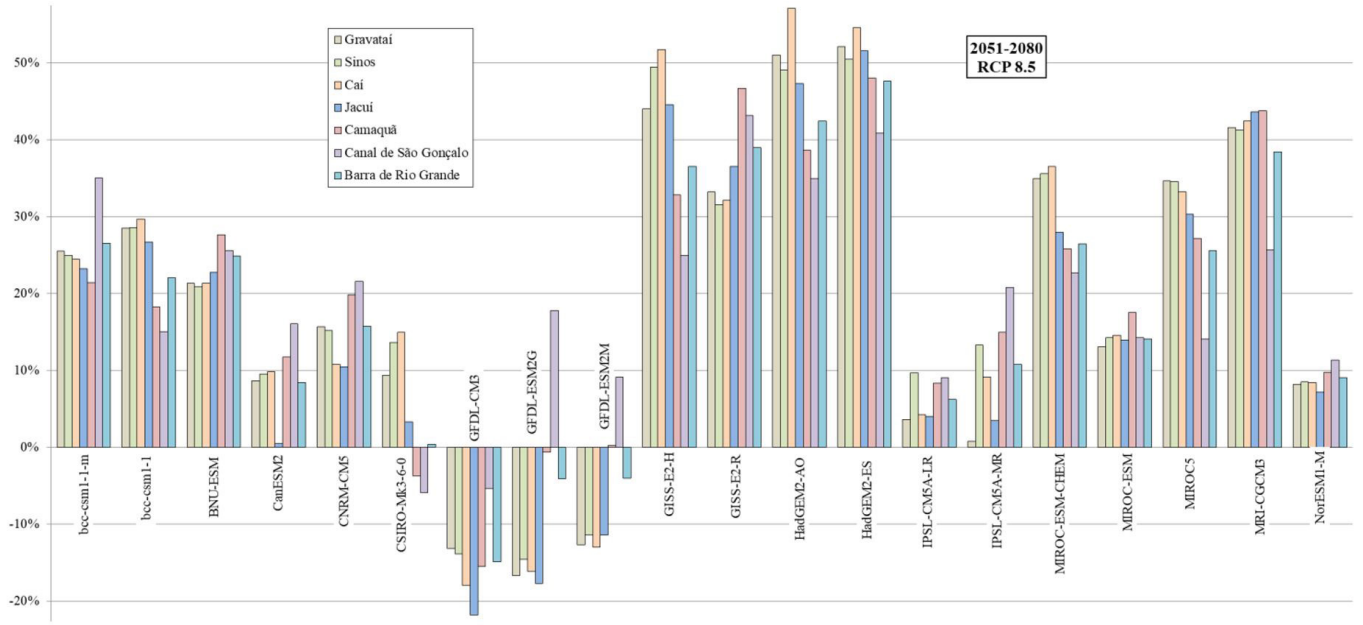

Figure 6. Average discharge variation at points of interest with RCP 8.5 over the 2051-2080 period.

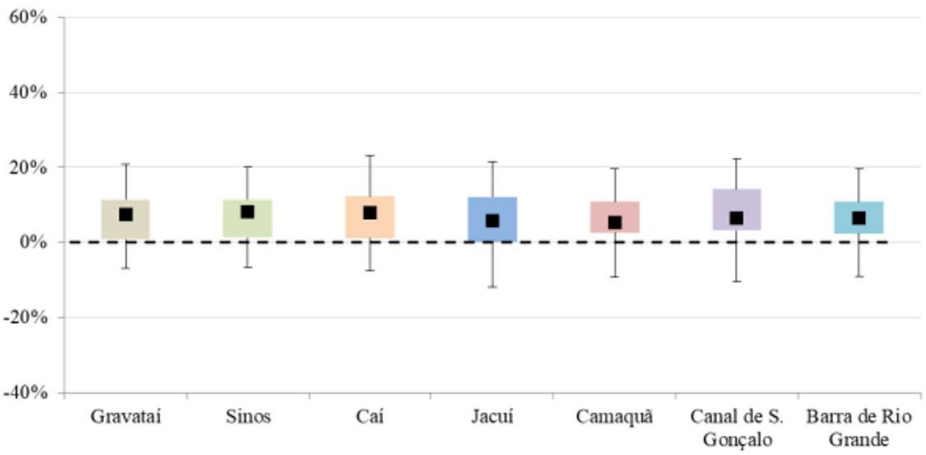

Figure 7. Box Plot Diagram for average discharge variation at points of interest with RCP 2.6 for the 2006-2035 period.

On Figure 8 it is noticeable that the diagram's highest whisker is larger in comparison to the lower, indicating that positive variations are more frequent and have a higher module in regards to negative variations. As for the Figure 9 graph, the lower whisker of the diagrams is slightly higher than the superior ones in some checkpoints, such as in the Jacuí River and the Camaquã River. However, as the rectangles are entirely above the zero axis, there is a predominance of positive discharge deviations.

In Figure 10, which represents the most extreme emissions scenario and the most distant future, the dispersion of values is greater, since the higher and lower whiskers of the diagrams are quite steep. It is, therefore, the scenario with the greatest uncertainties among the four evaluated.

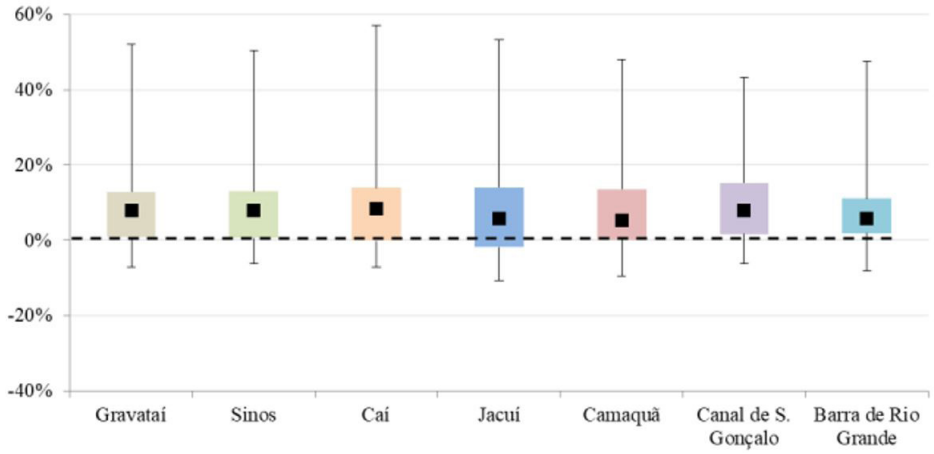

Figure 8. Box Plot Diagram for average discharge variation at points of interest with RCP 2.6 for the 2051-2080 period.

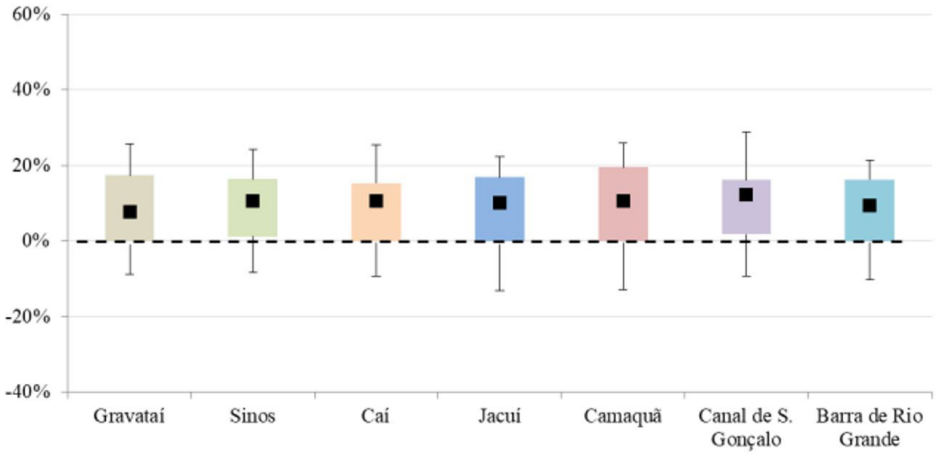

Figure 9. Box Plot Diagram for average discharge variation at points of interest with RCP 8.5 for the 2006-2035 period.

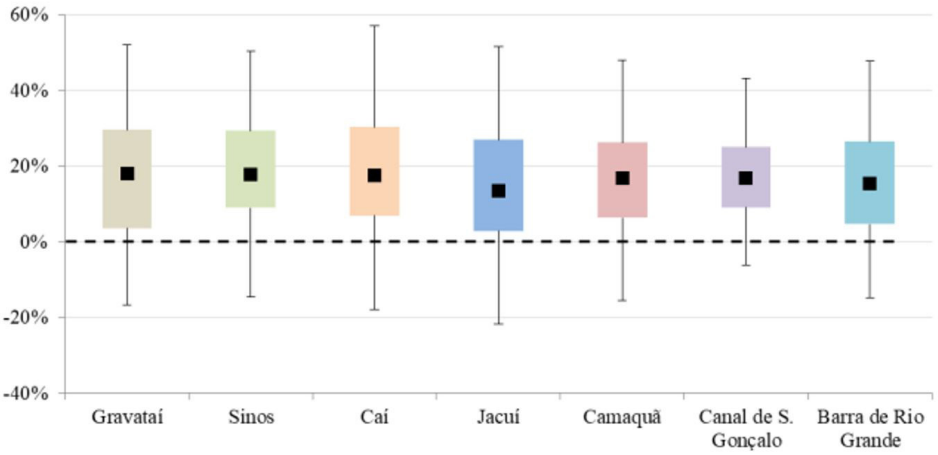

Figure 10. Box Plot Diagram for average discharge variation at points of interest with RCP 8.5 for the 2051-2080 period.

The presented graphs and diagrams allow for the verification that high emissions simulations (8.5) feature a greater variation in discharge range in relation to the control scenario, when compared to other discharge variations for the scenario with the highest GHG emissions mitigation (2.6). Also, the simulations for the period of the distant future (from 2051 to 2080) exhibit a higher discharge variation range when compared to the discharge variations generated for the near future (from 2006 to 2035). Therefore, the simulations for the 8.5 scenario and distant future are the ones that possess the highest dispersion in its results.

It is also noted that the largest part of the simulations generated positive discharge deviations in relation to the control scenario, that is, there are signs of a greater probability of increased discharge at the outflow point of the main rivers in the Patos Lagoon's catchments, as well as in the Lagoon's and Barra de Rio Grande. Observing the box plot diagrams for the 8.5, distant future scenario simulations, it is verified that the first and the third quartiles (consequently, the median) of the discharge deviation values are equal to or higher than zero. Indicating that the climate models of greater emissions and more distant future scenarios lead to a situation of greater discharge in the study region.

Table 4 features the climate models that presented the most extreme deviations at each checkpoint for each model and generated simulation.

Considering the 28 results for positive extremes illustrated in the table, future climate models that caused the greatest positive discharge deviations in average discharge were identified:

- HadGEM2-ES model, where 11 out of 28 specific average discharge results analyzed, was the one that featured the most extreme positive discharge deviation, being responsible for the highest positive discharge deviations in 5 out of the 7 analyzed checkpoints;
- HadGEM2-AO model, where 8 out of 28 specific average discharge results analyzed, was the one that presented the most extreme positive discharge variations, being responsible for the highest positive discharge deviations in 1 out of the 7 scrutinized checkpoints;
- MRI-CGCM3 model, where 6 out of 28 specific average discharge results analyzed, was the one that featured the most extreme positive discharge variations;
- GISS-E2-R model, where 3 out of the 28 specific average discharge results analyzed, was the model that featured the most extreme positive discharge deviations, it was also the model responsible for the greatest positive discharge variations in 1 out of 7 analyzed checkpoints.

Likewise, the climate models that resulted in simulations with the most expressive negative tendencies were pinpointed:

- GFDL-CM3 model, where 18 out of 28 specific average discharge results analyzed, was the model that presented the most extreme negative discharge deviations, being accountable for the most salient negative discharge deviations in 4 out of the 7 analyzed checkpoints;
- GFDL-ESM2M model, where 3 out of the 28 specific average discharge results analyzed, was the model that presented the most extreme negative discharge variations;
- CSIRO-Mk3-6-0 model, where 3 out of the 28 specific average discharge results analyzed, was the one that exhibited the most extreme negative discharge variations, being responsible for the most expressive negative discharge variations in 1 out of the 7 analyzed checkpoints;
- GFDL-ESM2G model, where 2 out of the 28 specific average discharge results analyzed, was the one that exhibited the most extreme negative discharge variations, being responsible for the most expressive negative discharge variations in 2 out of the 7 analyzed checkpoints;
- CanESM2 and MIROC-ESM models, where 1 out of the 28 specific average discharge results analyzed, were each the ones to feature the most extreme negative discharge variation values.

To assess one of the possible causes for the variability found in discharge variation results produced at each simulation, yearly rainfall averages within the evaluated basins were gauged, as well as the fluctuations of these average rains in each scenario

Table 4. Climate models that generated extreme discharge deviations for each simulated checkpoint.

Basin	Scenario	Period: 2006-2035		Period: 2051-2080	
		Extreme +	Extreme -	Extreme +	Extreme -
Gravataí	*RCP 2.6*	*HadGEM2-AO*	*GFDL-CM3*	*HadGEM2-AO*	*GFDL-ESM2M*
	RCP 8.5	*MRI-CGCM3*	*GFDL-CM3*	*HadGEM2-ES*	*GFDL-ESM2G*
Sinos	*RCP 2.6*	*HadGEM2-AO*	*GFDL-CM3*	*HadGEM2-AO*	*GFDL-ESM2M*
	RCP 8.5	*MRI-CGCM3*	*GFDL-CM3*	*HadGEM2-ES*	*GFDL-ESM2G*
Caí	*RCP 2.6*	*HadGEM2-AO*	*GFDL-CM3*	*HadGEM2-AO*	*GFDL-ESM2M*
	RCP 8.5	*MRI-CGCM3*	*GFDL-CM3*	*HadGEM2-AO*	*GFDL-CM3*
Jacuí	*RCP 2.6*	*HadGEM2-AO*	*GFDL-CM3*	*HadGEM2-ES*	*CanESM2*
	RCP 8.5	*MRI-CGCM3*	*GFDL-CM3*	*HadGEM2-ES*	*GFDL-CM3*
Camaquã	*RCP 2.6*	*MRI-CGCM3*	*GFDL-CM3*	*MRI-CGCM3*	*GFDL-CM3*
	RCP 8.5	*GISS-E2-R*	*GFDL-CM3*	*HadGEM2-ES*	*GFDL-CM3*
São Gonçalo Canal	*RCP 2.6*	*HadGEM2-ES*	*CSIRO-Mk3-6-0*	*HadGEM2-ES*	*MIROC-ESM*
	RCP 8.5	*GISS-E2-R*	*CSIRO-Mk3-6-0*	*GISS-E2-R*	*CSIRO-Mk3-6-0*
Barra de Rio Grande	*RCP 2.6*	*HadGEM2-ES*	*GFDL-CM3*	*HadGEM2-ES*	*GFDL-CM3*
	RCP 8.5	*HadGEM2-ES*	*GFDL-CM3*	*HadGEM2-ES*	*GFDL-CM3*

in relation to the average rainfall during the control period (from 1961 to 1990). Table 5 raised from this data, informing which climate model caused the greatest yearly average rainfall fluctuations in comparison to the control period, both in positive and in negative terms for each of the investigated basins. It is perceptible that in the vast majority of cases, a same climate model that originates the largest positive rain deviations, also provoked the greatest positive discharge deviations. The same goes for negative variations.

Spatial analysis

The Figure 11 chart presents the percentage of models that feature an increased discharge over the period of 2006 to 2035, considering a 2.6 RCP. Under these conditions, for the greater part of simulated water course reaches, between 70 and 80% of models mark an increase in discharge. Some reaches have between 80 and 90% of simulations pointing towards increased discharges, such as the northwest of Jacuí river basin and the extreme south of the São Gonçalo Canal basin.

The Figure 12's chart features the percentage of models pointing towards increased discharges at RCP 2.6 over the 2051 to 2080 period. In this scenario, the vast majority of reaches in the north portion of the simulated region (Jacuí River) have between 60 and 70% of models pointing towards an increase in discharges. The simulated region's middle portion contains between 70 and 80% of models indicating an increased discharge, while the southern section of the São Gonçalo Canal basin's Uruguayan side has between 80 and 90% of models pointing towards increased discharges.

The model percentages indicating increased discharges within the high greenhouse gases emissions scenario (RCP 8.5) over the 2006-2035 period are featured in the Figure 13's map. It is possible to observe in the map that Jacuí river basin and the lower portion of the Taquari-Antas river basin present an increased discharge probability of 60 to 70%. In the Uruguayan portion of the São Gonçalo Canal basin and in its southern Brazilian portion, the greater part of the reaches have between 80 and 90% of simulations pointing towards the increase of discharges.

The Figure 14's map presents the percentage of simulations indicating increased discharges over then 2051-2080 period, at RCP 8.5. It is visible that the probability of increased discharge is high in this scenario: between 80 and 90% across most simulated reaches, with the exception of Jacuí river basin and the lower portion of the Taquari-Antas basin, where the greater part of water reaches indicates an increased discharge probability between 70 and 80%. Over some reaches in the Uruguayan part of the São Gonçalo Canal basin, 100% of simulations indicate an increase in discharges.

The ensemble evaluation of these maps allows for the perception that across all water reaches, more than 60% of the

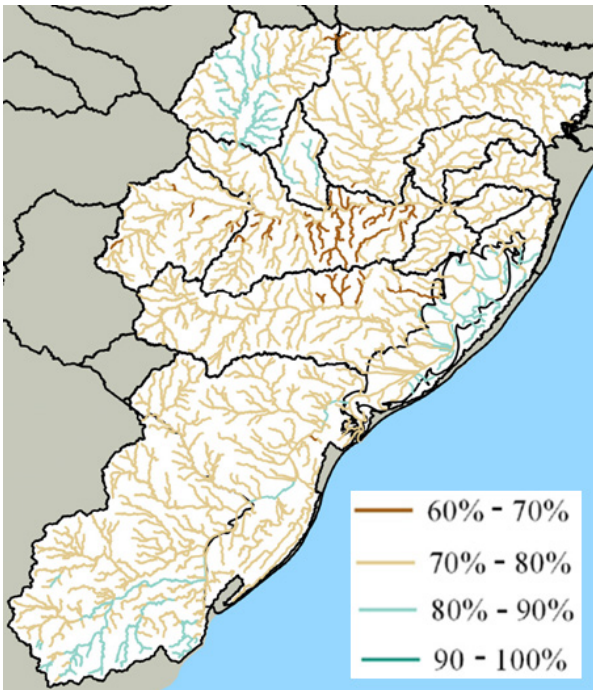

Figure 11. Percentage of the simulation ensemble pointing towards a discharge increase, at RCP 2.6 over the 2006-2035 period.

Table 5. Climate models that generated extreme rainfall fluctuations for each simulated control site.

Basin	Scenario	Period: 2006-2035		Period: 2051-2080	
		Extreme +	Extreme -	Extreme +	Extreme -
Gravataí	*RCP 2.6*	*HadGEM2-AO*	*GFDL-CM3*	*HadGEM2-AO*	*GFDL-ESM2G*
	RCP 8.5	*MRI-CGCM3*	*GFDL-CM3*	*HadGEM2-ES*	*GFDL-ESM2G*
Sinos	*RCP 2.6*	*HadGEM2-AO*	*GFDL-CM3*	*HadGEM2-AO*	*GFDL-CM3*
	RCP 8.5	*MRI-CGCM3*	*GFDL-CM3*	*HadGEM2-ES*	*GFDL-ESM2G*
Caí	*RCP 2.6*	*HadGEM2-AO*	*GFDL-CM3*	*HadGEM2-AO*	*GFDL-CM3*
	RCP 8.5	*MRI-CGCM3*	*GFDL-CM3*	*HadGEM2-AO*	*GFDL-ESM2G*
Jacuí	*RCP 2.6*	*HadGEM2-AO*	*GFDL-CM3*	*HadGEM2-ES*	*GFDL-CM3*
	RCP 8.5	*MRI-CGCM3*	*GFDL-CM3*	*HadGEM2-ES*	*GFDL-CM3*
Camaquã	*RCP 2.6*	*MRI-CGCM3*	*GFDL-CM3*	*MRI-CGCM3*	*GFDL-CM3*
	RCP 8.5	*MRI-CGCM3*	*GFDL-CM3*	*HadGEM2-ES*	*GFDL-CM3*
São Gonçalo Canal	*RCP 2.6*	*HadGEM2-ES*	*CSIRO-Mk3-6-0*	*HadGEM2-ES*	*MIROC-ESM*
	RCP 8.5	*bcc-csm1-1*	*CSIRO-Mk3-6-0*	*HadGEM2-ES*	*CSIRO-Mk3-6-0*
Barra de Rio Grande	*RCP 2.6*	*HadGEM2-ES*	*GFDL-CM3*	*HadGEM2-ES*	*GFDL-CM3*
	RCP 8.5	*HadGEM2-ES*	*GFDL-CM3*	*HadGEM2-ES*	*GFDL-CM3*

Obs: The table highlights climate models that do not coincide with extreme discharge variations displayed on Table 4.

performed simulation sets point to an increase in average discharge in relation to the control scenario, regardless of the RCP or period used. It is also verified that river reaches of the simulated region's southern portion, especially the basin contributing to the São Gonçalo Canal, are the ones that possess the highest probability of increased discharge when compared to the other simulated regions. In some river reaches of the São Gonçalo Canal basins, this percentage is higher than 80% for all studied periods and scenarios.

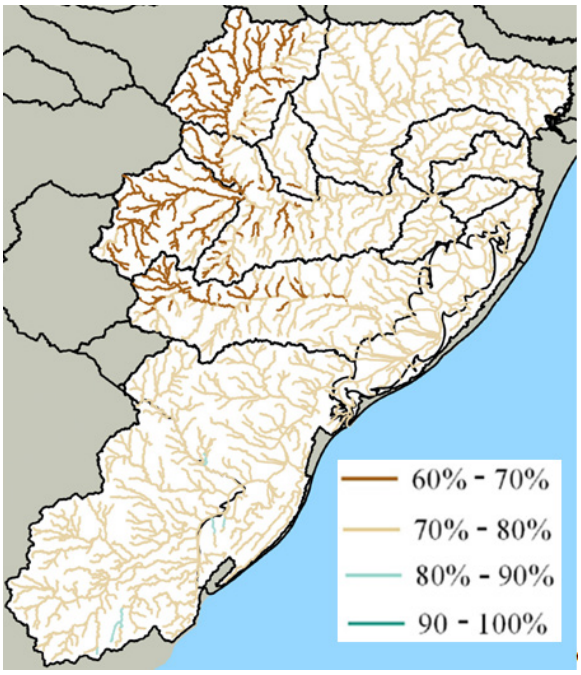

Figure 12. Percentage of the simulation ensemble pointing towards a discharge increase, at RCP 2.6 over the 2051-2080 period.

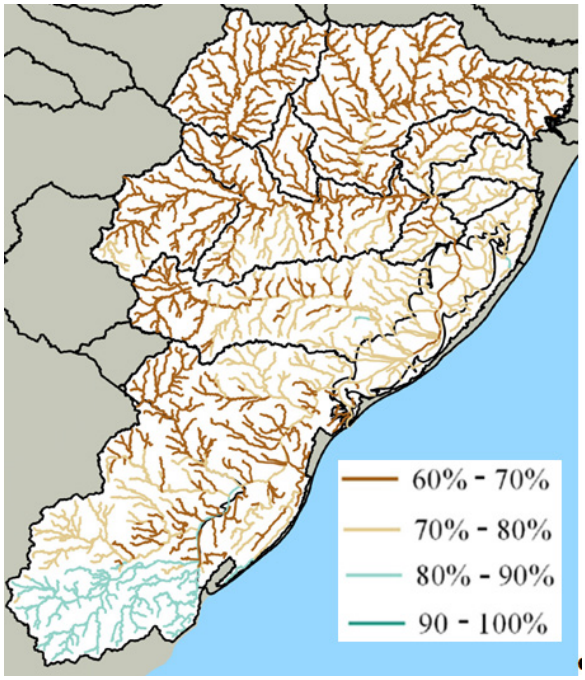

Figure 13. Percentage of the simulation ensemble pointing towards a discharge increase, at RCP 8.5 over the 2006-2035 period.

It is also remarked that, considering the rigorous greenhouse gases emissions mitigation scenario (RCP 2.6), the passage of time leads to a smaller tendency of increasing discharges, while in the scenario with severely high emissions (RCP 8.5), the passage of time causes an increase of this tendency.

From Figures 15-18 are presented the medians of average discharge variations in relation to the ensemble model control scenario, for each scenario and period. Figure 15's map displays the median results of generated variations considering RCP 2.6

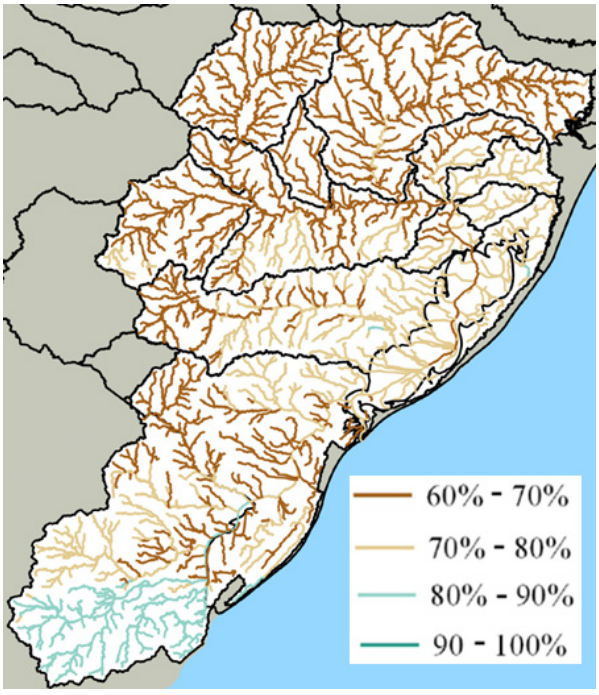

Figure 14. Percentage of the simulation enemble pointing towards a discharge increase, at RCP 8.5 over the 2051-2080 period.

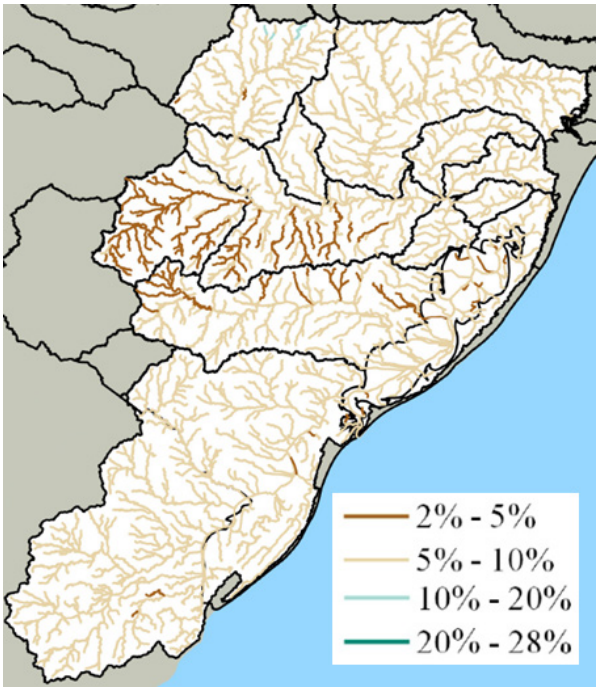

Figure 15. Ensemble simulations discharge variations medians, with RCP 2.6 over the 2006-2035 period.

and the 2006-2035 simulation period. In this scenario, the variation median of most river reaches is within the range of 5-10% discharge increase, with some stretches between 2-5%. At RCP 2.6 in the 2051-2080 period (Figure 16), the discharge variation median also stayed mostly in the range between 5-10% discharge increase, with some reaches between 2 and 5%.

In the Figure 17's map, where the RCP 8.5 medians are presented over the 2006-2035 period, a tendency towards more expressive positive discharge variations is evidenced in relation to what occurs in RCP 2.6 simulations, varying between 5-20%. Within this scenario, reaches with higher discharge deviations are located at the Camaquã River and São Gonçalo Canal basins; while lower deviations, between 5 and 10%, are found in water reaches of more northern basins.

Yet RCP 8.5 simulations for the more distant future (2051 to 2080), whose variation medians are featured in the map of Figure 18, are the ones that present the highest fluctuations among all studied scenarios. In this case, all simulations have a discharge increase median superior to 10%, reaching values higher than 20% increase in the northern region of the São Gonçalo Canal basins, as well as in the contributors to the right margin of Camaquã River.

While assessing the ensembled models' ensembles discharge variation medians maps, it is perceivable that for all simulations, regardless of the greenhouse gases emissions scenario, or the simulation period in question, the overall tendency is that of positive variations, that is, to increase average discharges, which varies between 2 and 28% in relation to the control scenario discharges. Once more, the passage of time in a scenario with a higher mitigation of GHG emissions indicates a decline in the increase of discharges, while the passage of time in scenarios with higher GHG emissions causes an aggravation in the discharge increase tendency.

Climate models that generated forecasts of average discharge increases higher than 40% in relation to the control scenario, and the hydrographic basins where these situations occur are pinpointed as follows:

- bcc-csm1-1m model: São Gonçalo Canal;
- GISS-E2-H model: Gravataí, Sinos, Caí, Jacuí river basins;
- GISS-E2-R model: Jacuí river, Camaquã, São Gonçalo Canal;

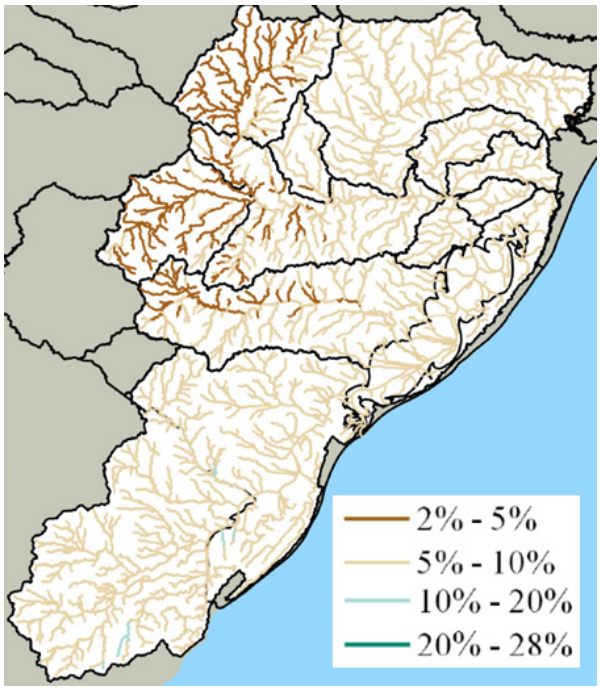

Figure 16. Ensemble simulations discharge variations medians, with RCP 2.6 over the 2051-2080 period.

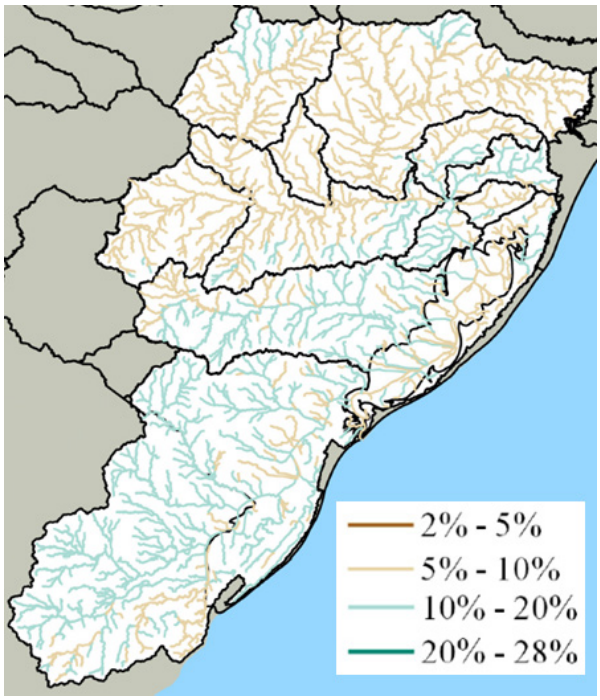

Figure 17. Ensemble simulations discharge variations medians, with RCP 8.5 over the 2006-2035 period.

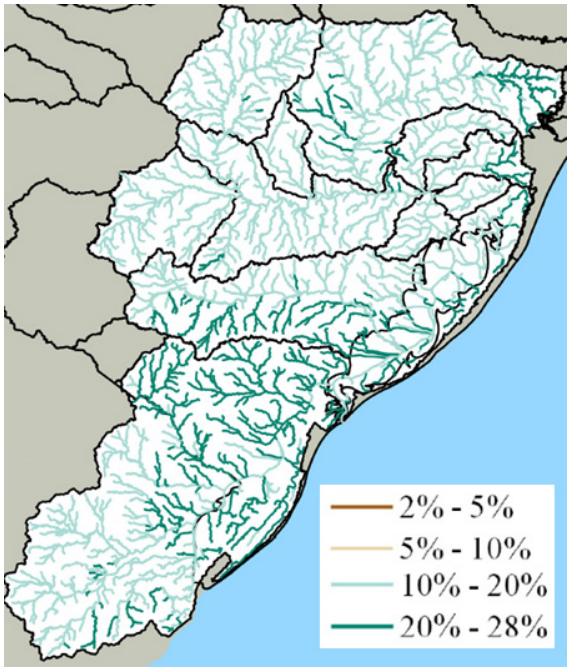

Figure 18. Ensemble simulations discharge variations medians, with RCP 8.5 over the 2051-2080 period.

- HadGEM2-AO and MRI-CGM3 models: Gravataí, Sinos, Caí, Jacuí and Camaquã river basins;
- HadGEM2-ES model: All basins.

Regarding the decline in discharge, the highlighted models are GFDL-CM3 and GFDL-ESM2G, which generated a decline in average discharge under -20% in relation to the current scenario within Jacuí river basin. It is emphasized that these conditions only arise with RCP 8.5 in the distant future period, from 2051 to 2080.

Table 6 was developed to assess one of the possible causes for spatial variability in the results of discharge variations, indicating the percentages of simulations that indicated negative or positive variations in yearly average rainfall and the median of these variations at each investigated hydrographic basin.

It is observed that in the more southern hydrographic basins, such as the Camaquã river and the São Gonçalo Canal, the amount of climate models that featured positive yearly average rainfall deviation is higher than that of the other basins. This information provides an explanation for results from Figures 15-18 that is, a greater amount of climate models induced an increase in forecast average rainfall for the future, engendering a higher amount of the hydrological model's simulations with increased average discharge.

However, it is verified that the yearly average rainfall medians in basins south of the study area are not the highest in the studied basin set, this information diverges from data presented on Figure 15. The expected outcome would be that, in basins with average variation medians higher than yearly rainfall averages, average discharge variations would also be higher. This goes to show that even when average rainfall does not raise so much, the positive discharge variations were much more expressive in basins south of the study area.

Extreme and average model analysis

In order to select climate models that supply the peak, bottom and average limits for the performed simulations, the medians of the results of each simulated model, scenario and period of every river reach were calculated. Afterwards, the square of the differences between the variations of each simulation was calculated in comparison to the ensemble median of each model, scenario and period for each unit-catchments. Table 7 presents the results of these calculated quadratic differences, added for every simulated river stretch. The last column of this table features the calculated average for the values of quadratic differences for each model.

Table 6. Percentage of simulations that featured negative or positive yearly rainfall averages and the median of these variations at each studied hydrographic basin.

Basin	Negative variation (%)	Positive variation (%)	Median (%)
Gravataí River	*21.3*	*78.8*	*5.7*
Sinos River	*21.3*	*78.8*	*7.9*
Caí River	*22.5*	*77.5*	*7.5*
Jacuí River	*22.5*	*77.5*	*6.7*
Camaquã River	*17.5*	*82.5*	*6.2*
São Gonçalo Canal	*13.8*	*86.3*	*7.0*

Table 7. Quadratic differences between each simulation's variations in contrast with the ensemble median for each period and scenario.

RCP	2.6		8.5		Average
Period	2006-2035	2051-2080	2006-2035	2051-2080	
bcc-csm1-1-m	*12.3*	*35*	*38.7*	*27.6*	*28.4*
bcc-csm1-1	*7.1*	*5.4*	*6.3*	*17*	*9*
BNU-ESM	*4.2*	*11.6*	*14.6*	*11.1*	*10.4*
CanESM2	*34.9*	*49.4*	*60.5*	*48.7*	*48.4*
CNRM-CM5	*5.7*	*10.2*	*14.8*	*8.1*	*9.7*
CSIRO-Mk3-6-0	*46.1*	*10.7*	*68.3*	*118.6*	*60.9*
GFDL-CM3	*63.9*	*62*	*106*	*310.3*	*135.6*
GFDL-ESM2G	*32.5*	*28.5*	*21.2*	*199.2*	*70.4*
GFDL-ESM2M	*8.7*	*27*	*36.6*	*151.4*	*55.9*
GISS-E2-H	*7.1*	*3.2*	*13.5*	*100.4*	*31*
GISS-E2-R	*21.3*	*10.1*	*46.4*	*119.1*	*49.3*
HadGEM2-AO	*36.2*	*70.5*	*11.5*	*157.9*	*69*
HadGEM2-ES	*50.3*	*76*	*36.6*	*216.6*	*94.9*
IPSL-CM5A-LR	*8*	*11.4*	*5.9*	*49.2*	*18.6*
IPSL-CM5A-MR	*11.6*	*11.5*	*7.5*	*35.8*	*16.6*
MIROC-ESM-CHEM	*1.2*	*19.6*	*26.5*	*22.7*	*17.5*
MIROC-ESM	*13.9*	*25.5*	*12.2*	*11.9*	*15.9*
MIROC5	*8.6*	*21.4*	*12.2*	*33.7*	*19*
MRI-CGCM3	*48.2*	*53*	*29.7*	*115.3*	*61.6*
NorESM1-M	*1.3*	*3.5*	*32*	*30.5*	*16.8*

Table 8. Sums of the differences between each simulation's variation in contrast with the ensemble median of each period and scenario.

RCP	2.6		8.5	
Period	2006-2035	2051-2080	2006-2035	2051-2080
bcc-csm1-1	*89.3*	*65.7*	*-53.6*	*54.4*
bcc-csm1-1-m	*170.1*	*288.1*	*286.1*	*206.2*
BNU-ESM	*74.7*	*-54.0*	*182.6*	*146.4*
CanESM2	*-264.9*	*-315.2*	*-363.6*	*-274.8*
CNRM-CM5	*-80.8*	*-69.2*	*-61.5*	*-87.8*
CSIRO-Mk3-6-0	*-278.0*	*-113.3*	*-380.8*	*-513.4*
GFDL-CM3	*-391.7*	*-392.3*	*-513.2*	*-874.3*
GFDL-ESM2G	*-32.8*	*-59.2*	*-47.2*	*-558.2*
GFDL-ESM2M	*-127.6*	*-216.1*	*-301.1*	*-573.1*
GISS-E2-H	*-11.7*	*-51.8*	*138.4*	*421.9*
GISS-E2-R	*199.7*	*70.4*	*251.2*	*531.5*
HadGEM2-AO	*278.4*	*426.6*	*115.8*	*585.9*
HadGEM2-ES	*356.9*	*438.4*	*302.0*	*727.9*
IPSL-CM5A-LR	*21.5*	*6.7*	*-19.7*	*-316.0*
IPSL-CM5A-MR	*48.1*	*-1.4*	*38.5*	*-196.1*
MIROC5	*88.8*	*191.1*	*131.6*	*134.1*
MIROC-ESM	*-184.6*	*-227.5*	*131,6*	*-136.6*
MIROC-ESM-CHEM	*-41.9*	*-214.8*	*-257.5*	*176.7*
MRI-CGCM3	*337.3*	*349.3*	*236.5*	*478.0*
NorESM1-M	*-45.9*	*41.2*	*-284.6*	*-269.1*

Table 7 shows that, for the RCP 2.6 simulation in the near-future period, the models that exhibit the smaller differences are MIROC-ESM-CHEM and NorESM1-M. This last one also presents small differences for the distant future at RCP 8.5, however the model with the smallest difference in this scenario is GISS-E2-H.

For simulations at RCP 8.5, the models with the smallest disparities are IPSL-CM5A-LR and bcc-csm1-1 for the near-future, and CNRM-CM5 e BNU-ESM models, for the distant future. These models with small disparities are the ones that represent variation values near the median variation value for all of the performed simulations. The final column in Table 7 reports the quadratic difference average for all periods and scenarios, and allows for the inference that models bcc-csm1-1, BNU-ESM and CNRM-CM5 are the ones with the smallest absolute difference average values in relation to the median. Yet, the models whose values are displayed in the last column of Table 7 are high, being the ones that represent extreme variations, both positive as well as negative. The models with higher absolute average differences are GFDL-CM3 and HadGEM2-ES.

Seeing as Table 7 does not allow for the identification of whether the deviations are positive or negative, the data was evaluated following this approach: differences were calculated between the medians of each model's set and results of each simulation for every river stretch. Table 8 presents these differences added for every river stretch of each simulation.

Table 8 grants the observation that the GFDL-CM3 model presents the highest negative differences, and the HadGEM2-ES model presents the highest positive differences for every simulated period and scenario. Therefore, they are the models that provide scenarios of low and high discharges, respectively, according to the aforementioned in previous items.

CONCLUSIONS

The influence of future climate change scenarios in water availability was assessed for the rivers that drains into the Patos Lagoon, contemplating various scenarios projected by global models from the 5th IPCC report. It was possible to verify a tendency towards the increase of discharges in the simulated region. Most of the climate models evaluated indicated at least some percentage of average discharge increase across all modeled discretization units.

Furthermore, the medians of these average discharges in relation to the control scenario are positive in all simulated scenarios. This conclusion converges with the results published by Lima et al. (2014) and Pachauri & Meyer (2014), which verify a predominance of forecasts of increased discharge for the South region of Brazil, stemming from five AR5 climate models. As there are no other studies similar to this one in the Patos Lagoon watershed, it is not possible to present other comparisons with literature.

In the current study, the percentage of ensemble simulations that generated positive variations in average discharges stayed within the 60 to 100% range, taking the entire set of performed simulations into account. The calculated intermediate increase of average discharge remained in the 2 to 28% range in relation to the simulated control scenario; the yearly rainfall average median being around 7%. A greater tendency towards increased discharges in southernmost watercourses within the study area, such as in the River Camaquã and São Gonçalo Canal basins, especially in the distant-future period (from 2051 to 2080), with RCP at 8.5. In northernmost hydrographic basins, the amount of models indicating increased discharges is smaller than the set's median increase, contrasted with the results of the two aforementioned basins.

The analysis of the simulation results allowed for the specification of the most suitable climate models for this purpose. The HadGEM2-ES climate model simulations were the ones

that presented a greater tendency to increase discharge, and the simulations with the GFDL-CM3 model were the ones to exhibit a greater tendency to decrease discharge. The ensemble evaluation of the results generated by these two models, associated to the high GHG emissions scenario (RCP 8.5) is capable of creating extreme discharge scenarios, - both maximal and minimal - that are forecast for the future contemplating climate changes in the Patos Lagoon's basin. For the acquisition of scenarios representing the ensemble median of the observed discharges in future projections, the most suitable models are bcc-csm1-1, BNU-ESM and CNRM-CM5.

Concerning the identification of regions where the largest effects are projected, Jacuí river basin is the one where the largest variation ranges were detected. In other words, this region possesses highest sensitivity to climate changes forecast by CMIP5 global models published in the AR5.

Considering that future climate data used in this study has high uncertainty, we emphasize that the results of discharge variations presented for simulated future scenarios should be considered as trends, not as absolute data. In addition, we recommend the evaluation of precipitation, temperature and evapotranspiration anomalies, to be able to jointly compare and evaluate the climate variables and the discharge.

REFERENCES

Adam, K. N., & Collischonn, W. (2013). Análise dos impactos de mudanças climáticas nos regimes de precipitação e vazão na bacia hidrográfica do rio Ibicuí. *Revista Brasileira de Recursos Hídricos*, *18*(3), 1-11. http://dx.doi.org/10.21168/rbrh.v18n3.p69-79.

Adam, K. N., Fan, F. M., Pontes, P. R., Bravo, J. M., & Collischonn, W. (2014, setembro). Climate change and floods in Paraná river basin. In *Proceedings of The 6th International Conference in Flood Management (pp. 1-10)*. São Paulo: ICFM6.

Alvarenga, L. A., Mello, C. R., Colombo, A., Cuartas, L. A., & Chou, S. C. (2016). Respostas hidrológicas de uma bacia hidrográfica de cabeceira às mudanças climáticas. *Ciência e Agrotecnologia*, *40*(6), 647-657. http://dx.doi.org/10.1590/1413-70542016406027716.

Amorim, P. B., & Chaffe, P. B. (2019). Towards a comprehensive characterization of evidence in synthesis assessments: the climate change impacts on the Brazilian water sources. *Climatic Change, 155(1), 37-37. http://dx.doi.org/10.1007/s10584-019-02430-9*.

Borges, P. B., & Chaffe, P. L. B. (2019). Integrating climate models into hydrological modelling: what's going on in Brazil. *Revista Brasileira de Recursos Hídricos*, *24*(1), 1-11.

Brasil. (1997, 09 de janeiro). Lei nº 9.433, de 8 de janeiro de 1997. *Diário Oficial da União*. Brasília.

Bravo, J. M., Collischonn, B., Paz, A. R., Allasia, D. G., Domecq, F. (2014). Impact of projected climate change on hydrologic regime of the Upper Paraguay River basin. *Climatic Change*, 127:27. http://dx.doi.org/10.1007/s10584-013-0816-2.

Ceará. (1992, 24 de julho). Lei nº 11.996, de 24 de julho de 1992. *Diário Oficial do Estado*. Fortaleza.

Fernandes, R. O., Silveira, C. S., Studart, T. M. C., & Souza Filho, F. A. (2017). Intercomparação das vazões regularizadas de grandes reservatórios da bacia do Rio Jaguaribe-CE em cenários de mudanças climáticas. *Revista Brasileira de Recursos Hídricos*, *22*(1), e11.

Lima, J. W. M., Collischonn, W., & Marengo, J. A. (2014). *Efeitos das mudanças climáticas na geração de energia elétrica*. São Paulo: AES Tietê.

Lopes, V. A. R. (2017). *Modelagem hidrológica e hidrodinâmica integrada de bacias e sistemas lagunares com influência do Vento* (Dissertação de mestrado). Universidade Federal do Rio Grande do Sul, Porto Alegre.

Lopes, V. A. R., Fan, F. M., Pontes, P. R. M., Siqueira, V. A., Collischonn, W., & Motta Marques, D. (2018). A first integrated modelling of a river-lagoon large-scale hydrological system for forecasting purposes. *Journal of Hydrology (Amsterdam), 565, 177-196. http://dx.doi.org/10.1016/j.jhydrol.2018.08.011*.

Nóbrega, M. T., Collischonn, W., Tucci, C. E. M., & Paz, A. R. (2011). Uncertainty in climate change impacts on water resources in the Rio Grande Basin, Brazil. *Hydrology and Earth System Sciences, 15(2), 585-595*. http://dx.doi.org/10.5194/hess-15-585-2011.

Oliveira, V. A., Mello, C. R., Viola, M. R., & Srinivasan, R. (2017). Assessment of climate change impacts on streamflow and hydropower potential in the headwater region of the Grande river basin, Southeastern Brazil. *International Journal of Climatology, 37(15), 5005-5023*. http://dx.doi.org/10.1002/joc.5138.

Pachauri, R. K., & Meyer, L. A. (Eds.), (2014). *Climate Change 2014: systhesis report (Contributions of Working Groups I, II and III to the Fifth Assessment Report of the IPCC, Core Writing Team, 151 p.)*. Geneva: Intergovernmental Panel on Climate Change.

Pereira, M., Kayser, R. H. B., & Collischonn, W. (2012). Integração do Modelo Hidrológico para Grandes Bacias MGB-IPH e Sistemas de Informação Geográfica para suporte à decisão de outorga de direito de uso da água. *Revista de Gestão de Águas da América Latina*, *9*, 21-33.

Rio Grande do Sul. (1995, 01 de janeiro). Lei nº 10.350 de 30 de dezembro de 1994. *Diário Oficial do Estado*. Porto Alegre.

São Paulo. (1991, 30 de dezembro). Lei nº 7.663, de 30 de dezembro de 1991. *Assessoria Técnico-Legislativa*. São Paulo.

Sorribas, M. V., Paiva, R. C. D., Melack, J. M., Bravo, J. M., Jones, C., Carvalho, L., Beighley, E., Forsberg, B., & Costa, M. H. (2016). Projections of climate change effects on discharge and inundation in the Amazon basin. *Climatic Change, 136(3-4), 555-570*. http://dx.doi.org/10.1007/s10584-016-1640-2.

Tejadas, B. E., Bravo, J. M., Sanagiotto, D. G., Tassi, R., & Marques, D. M. L. M. (2016). Projeções de Vazão Afluente à Lagoa Mangueira com Base em Cenários de Mudanças Climáticas. *Revista Brasileira de Meteorologia*, *31*(3), 1-11. http://dx.doi.org/10.1590/0102-778631320150139.

Authors contribution

Raíza Cristóvão Schuster: Paper's lead author, partial requirement to obtain Master's degree in Water Resources and Environmental Sanitation at Universidade Federal do Rio Grande do Sul.

Fernando Mainardi Fan: Lead author's advisor.

Walter Collischonn: Lead author's co-advisor.